



Chapter 2

Magnet requirements in circular accelerators: the interaction regions

Plan of the chapter

In this chapter we discuss the magnet requirements in the interaction regions. We first introduce the definition of luminosity (section 2.1), summarizing the main physical effects that sets limits to high luminosities (section 2.2). In section 2.3 we outline the requirements on the experimental magnets; the longitudinal size of the experiment is an essential parameter for the optics around the interaction region. In section 2.4 we present the layout for the separation and recombination dipoles in a collider with separate beam pipes. We then discuss the need of a crossing angle to avoid parasitic beam collisions in section 2.5, and its adverse effect on luminosity via the geometric reduction factor. Finally, in section 2.6 we discuss the optics around the collision points, showing the requirements in terms of gradients, aperture and length for a triplet system aiming at minimizing the beam size in the interaction point. The whole chapter is focussed on the case of LHC and HL-LHC.

2.1 Luminosity of a collider

Besides the energy, the other relevant parameter of a circular collider is the luminosity, which is related to the quantity of collisions per second. Luminosity L is expressed in $\text{cm}^{-2} \text{s}^{-1}$, and not simply in s^{-1} (collisions per second), since for a given collider events with larger probability will give more collisions [1]. The probability associated to a given type of collisions is expressed as a cross-section, that intuitively can be imagined as the surface of the colliding particle. The number of events per second is then the product between the luminosity and the cross-section of that event. Cross-sections are expressed in barns, where $1 \text{ barn} = 10^{-24} \text{ cm}^2$, i.e. is a square of 10^{-14} m . Typically for the proton-proton cross-section at the LHC 7+7 TeV energy the cross-section is of the order of 0.1 barn: therefore the colliding particles have a “size” that is $0.3 \times 10^{-14} \text{ m}$. In Appendix B we will show that the size of the atom is of the order of $0.5 \times 10^{-10} \text{ m}$: therefore we are four order of magnitudes below the atom size. Indeed, $0.3 \times 10^{-14} \text{ m}$ is the scale of the classical radius of the electron, defined as the size of a charged particle whose electrostatic energy is equal to the rest energy mc^2 . For the LHC [2], the inelastic cross-section of proton collisions at 7 TeV is $\sim 0.06 \text{ barn}$, the nominal luminosity is $10^{34} \text{ cm}^{-2} \text{ s}^{-1}$, and therefore we have about 6 billions of collisions per second

The luminosity is a characteristic of the accelerator, independent of the collision type. It is given by

$$L = \frac{n_b N_b^2 f_{rev} \gamma_r}{4\pi \epsilon_n \beta^*} F(\beta^*); \quad (2.1)$$

where we have

- Main parameters of the collider: γ_r is the relativistic factor of the collision energy, and f_{rev} is the frequency of the accelerator, i.e. the particle velocity divided by the accelerator length;
- Beam parameters: the beam is not continuous, but separated in n_b bunches, each containing N_b particles per bunch;
- Injector features: ε_n is the emittance of the beam in collision, which has been introduced in chapter 1. It is given by the injection emittance, plus some increase (emittance blow-up) given by the dynamics of the collider;
- Collider optics: β^* is the beta function in the interaction point (the so called beta-star, see section 2.6). F is a geometrical factor that will be discussed in section 2.5.

Luminosity is usually given in CGS units, i.e. $\text{cm}^{-2} \text{s}^{-1}$, whereas engineers and applied physicists usually use International System (SI) or mixed units, typically either m or cm for β^* , and mm mrad for the emittance. The safest choice is to use SI units and to avoid mixing units when possible, as we do here - when we had exceptions as for the energy in GeV in the previous chapter, we explicitly state the units. So, luminosity of Eq. (2.1) provides values in $\text{m}^{-2} \text{s}^{-1}$ and not in $\text{cm}^{-2} \text{s}^{-1}$.

To increase luminosity there are two main paths: (i) collide more particles; note that the dependence on particles per bunch N_b is quadratic; (ii) reduce the size of the beam in the collision, i.e. $\varepsilon_n \beta^*$; this can be done either through decreasing the emittance of the injectors or by having an optics that allows smaller beta functions in the interaction points. Note that there is also a dependence on the main collider parameters: luminosity is (i) proportional to the energy through the gamma factor, and (ii) is inverse proportional to the collider size, through the frequency. A summary of the luminosity parameters for several colliders is given in Table 2.1.

Table 2.1: Summary of main luminosity parameters of some colliders

Particle	Tevatron		HERA		LHC nom.	LHC 2013	LHC 2020	HL-LHC
	p+	p-	p+	e-	p+	p+	p+	p+
E (GeV)	900		820	30	7000	4000	6800	7000
l (km)	6.28		6.4		27.6	27.6	27.6	27.6
N_b (adim)	7.00E+10	2.90E+10	3.60E+10	1.01E+11	1.15E+11	1.35E+11	1.40E+11	2.20E+11
n_b (adim)	6	6	210	210	2808	1404	2500	2760
γ_r (adim)	958		872	55080	7448	4256	7235	7448
f_{rev} (s^{-1})	4.78E+04		4.70E+04		1.09E+04	1.09E+04	1.09E+04	1.09E+04
β^* (m)	0.55		2.2	10	0.55	0.6	0.3	0.15
F (adim)	0.71		1	1	0.86	0.9	0.54	0.716
ε_n (m)	4.20E-06	3.00E-06	1.00E-05	1.00E-05	3.75E-06	2.20E-06	2.20E-06	2.50E-06
L ($\text{cm}^{-2} \text{s}^{-1}$)	1.6E+30		5.30E+36		1.0E+34	6.42E+33	2.5E+34	1.6E+35
L_{level} ($\text{cm}^{-2} \text{s}^{-1}$)							2.5E+34	5.0E+34
θ (μrad)					150	150		300
σ_{in} (mbarn)					60	60	60	60
$Pile-up$ (adim)					20	25	55	100

Accelerators can collide the same particle type, as the LHC: in this case the counter-rotating beams require opposite magnetic fields, i.e the magnets shall have a double aperture, and the dipoles shall provide opposite fields in each aperture. This is doubling the magnet system. The other option is to collide particle and antiparticle (as Tevatron [3]): in this case the two beams can circulate in the same pipe, and profit of the same magnetic field. They rotate in opposite directions since their charge is opposite. The two beams are sent along spirals, centered on the magnet axis, so to avoid that they

collide in each section of the machine. The spirals are collapsed on each other in the experiments. Luminosity equation reads

$$L = \frac{n_b N_b^+ N_b^- f_{rev} \gamma_r}{4\pi \sqrt{\epsilon_n^+ \beta^{*+}} \sqrt{\epsilon_n^- \beta^{*-}}} F(\beta^{*+}, \beta^{*-}); \quad (2.2)$$

where N^+ is the number of particles per bunch and N^- is the number of antiparticles, and emittance and β^* can have different values for the two types of beams. The disadvantage is that generating high intensity bunches of antiparticles is not trivial; Tevatron luminosity has always been limited by the number of antiprotons.

Example 2.1: Compute the collisions per second in the LHC, if it was filled with cherries instead of protons, assuming the nominal luminosity $10^{34} \text{ cm}^{-2} \text{ s}^{-1}$. Assuming for the cherry cross-section 1 cm^2 , one would have 10^{34} collisions per second.

Example 2.2: Compute the energy stored in one nominal LHC beam; express this energy in units of chemical energy stored in a BigMac.

The energy of the beam is given by

$$U_{beam} = n_b N_b E = 2808 \times 1.15 \times 10^{11} \times 7 \times 10^{12} \times 1.602 \times 10^{-19} = 360 \text{ MJ} \quad (2.3)$$

Since one BigMac has $\sim 500 \text{ kcal}$, i.e., $\sim 2 \text{ MJ}$ ($1 \text{ cal} = 4.18 \text{ J}$), the beam is equivalent to ~ 180 BigMacs.

Example 2.3: Considering that the LHC complex has a power consumption of a maximum of 200 MW, and that the accelerator is refilled every 12 hours, estimate the efficiency of the LHC in concentrating the grid power in protons. Estimate the maximum efficiency, considering a continuous refilling and acceleration.

The power given to the protons (two beams) is

$$P_{beam} = \frac{2E_{beam}}{12 \text{ hours}} = \frac{2 \times 360 \times 10^6}{43200} = 17 \text{ kW}. \quad (2.4)$$

So since the LHC complex consumes $\sim 200 \text{ MW}$, the efficiency is the energy concentration is of the order of 1:10000. Considering that the acceleration takes about 1000 s, and the injection and ramp down another 2000 s, in principle one could accelerate every hour, and the power given to the beams would be 200 kW. In these conditions, there is a factor 1:1000 in the efficiency.

2.2 Luminosity limitations

There are several physical phenomena that limit luminosity; before focusing on the requirements on the insertion region magnets we will briefly recall a few of them.

Limitations due to beam-beam tune shift; when the beams collide, one proton sees the electrostatic field of the other bunch, which is proportional to the density of charges in the transverse plane. Beyond a threshold of this density, the Coulomb interaction creates a tuneshift that makes the beam unstable: this puts an limit on the ratio between the bunch intensity and the emittance N_b/ϵ_n (defined as the beam brilliance). The beam-beam tune shift parameter [1] is defined as

$$\xi \equiv n_{IP} \frac{r_p N_b}{4\pi \epsilon_n}; \quad (2.5)$$

where r_p is the classical radius of the proton (see also Appendix B for the definition),

$$r_p \equiv \frac{e^2}{4\pi\epsilon_0 m_p c^2} = \frac{(1.602 \times 10^{-19})^2}{4\pi \times 8.85 \times 10^{-12} \times 1.672 \times 10^{-27} \times (3 \times 10^8)^2} = 1.53 \times 10^{-18} \text{ m} \quad (2.6)$$

and n_{IP} is the number of interaction point. This empirical limit is usually set at 0.01, and depends on nonlinearities in the transverse motion (the less the nonlinearities, the larger the beam-beam limit). Please note that we are using the slightly misleading notation ϵ_n for transverse beam emittance, and ϵ_0 for the vacuum permittivity.

Example 2.4: Estimate the beam-beam tune shift for the nominal LHC and for the 2015 run [4], using data of Table 1.

The beam-beam tune shift for the nominal parameters (see Table 1) is given by

$$\xi \equiv n_{IP} \frac{r_p N_b}{4\pi\epsilon_n} = 2 \frac{1.53 \times 10^{-18}}{4\pi} \frac{1.15 \times 10^{11}}{3.75 \times 10^{-6}} = 0.0075 \quad (2.7)$$

and becomes 0.02 for the parameters used in the 2015 run, thanks to the 30% smaller emittance and to the 50% larger beam population:

$$\xi = 2 \frac{1.53 \times 10^{-18}}{4\pi} \frac{1.7 \times 10^{11}}{2.2 \times 10^{-6}} = 0.019. \quad (2.8)$$

This is twice what is considered as a safe limit for beam-beam. The LHC successfully operated with this high brilliance thanks to the low level and to the good control of the accelerator nonlinearities.

Limitations due to the electron cloud: when the bunches are too closely spaced, the electrons of the beam screen that are extracted by the particles in the beam halo can be accelerated by the next bunch, thus extracting other electrons and creating an electron cloud in the beam pipe through an avalanche effect (see Fig. 2.1). This effect, discovered in the 80's [5], is related to the bunch intensity and to the number of bunches; it can be partially cured by a treatment of the beam screen surface to reduce the probability of extracting electrons. The electron cloud sets a lower bound on the bunch spacing.

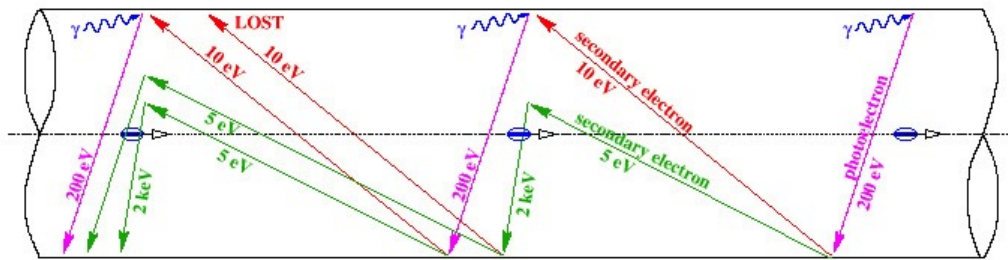


Fig. 2.1: Mechanism of electron cloud formation

Limitations due to the synchrotron radiation: a charged particle going through a bending dipole emits radiation, and the energy loss per turn is given by

$$E_s = \frac{e^2 \gamma_r^4}{3\epsilon_0 \rho} \quad (2.9)$$

where ρ is the dipole bending radius. The energy loss per turn scales with the fourth power of the relativistic gamma and with the inverse of the curvature radius. In many texts you will see equations where the gamma factor is replaced by the ratio between the particle energy and the mass.

$$E_s = \frac{e^2}{3\epsilon_0} \frac{E^4}{(mc^2)^4 \rho}. \quad (2.10)$$

This shows that for a given energy the power loss scales with the inverse of the fourth power of the mass. This is why proton colliders present the advantage with respect to electron colliders of having $\sim 10^{13}$ smaller energy loss. A relevant quantity for the cryogenics is the power loss per meter:

$$P_s = n_b N_b \frac{E_s f}{L_T} \approx n_b N_b \frac{E_s c}{L_T^2} = n_b N_b \frac{e^2 c}{3\epsilon_0 L_T^2} \frac{\gamma_r^4}{\rho}. \quad (2.11)$$

The main limitation here is given by the cryogenic power required to remove this heat from the beam screen and from the magnet.

Example 2.5: Compute the energy loss per turn and per particle, and the power loss per meter in the LHC [2], in the FCC-hh study [6], and in the LEP [7].

In the LHC the energy loss per turn is given by

$$E_s = \frac{(1.602 \times 10^{-19})^2}{3 \times 8.85 \times 10^{-12}} \frac{7450^4}{2801} = 1.06 \times 10^{-15} \text{ J} \quad (2.12)$$

and the power loss per meter is

$$P_s = 2808 \times 1.15 \times 10^{11} \frac{1.06 \times 10^{-15} \times 3 \times 10^8}{26700^2} = 0.144 \text{ W/m}. \quad (2.13)$$

For the FCC the energy loss per particle per turn is ~ 700 times larger, since the length is four times larger, and the energy 7 times larger (scales with γ_r^4/L_T)

$$E_s = \frac{(1.602 \times 10^{-19})^2}{3 \times 8.85 \times 10^{-12}} \frac{53200^4}{10400} = 7.4 \times 10^{-13} \text{ J} \quad (2.14)$$

and the power loss per meter is ~ 170 times larger (scales with γ_r^4/L_T^2)

$$P_s = 10400 \times 1.15 \times 10^{11} \frac{7.4 \times 10^{-13} \times 3 \times 10^8}{26700^2} = 26.7 \text{ W/m}. \quad (2.15)$$

For the LEP, accelerating electrons at 115 GeV, one has

$$E_s = \frac{(1.602 \times 10^{-19})^2}{3 \times 8.85 \times 10^{-12}} \frac{225000^4}{3030} = 8.13 \times 10^{-10} \text{ J} \quad (2.16)$$

and the power loss per meter is

$$P_s = 3030 \times 2 \times 10^{11} \frac{8.13 \times 10^{-10} \times 3 \times 10^8}{26700^2} = 207 \text{ W/m}. \quad (2.17)$$

Limitations due to the beta function in the interaction point: one can prove (see Appendix A) that in the experimental region around the interaction point, where no transverse fields are present, the beta function has the following parabolic form

$$\beta(s) = \beta^* + \frac{s^2}{\beta^*} \quad (2.18)$$

where $s=0$ is the interaction point in the centre of the experiment. Therefore in the first magnets seen by the beam after the collisions, which are at a distance l^* , the beta function is proportional to the inverse of β^* .

$$\beta(l^*) = \beta^* + \frac{l^{*2}}{\beta^*} \approx \frac{l^{*2}}{\beta^*}. \quad (2.19)$$

This relation has a deep physical meaning: if we want to reduce the beam size in the interaction point via a reduction of the beta function, we must have very large aperture magnets close to the experiments. The possibility of approaching the first magnets (reducing l^*) is not viable, since the experimental magnets need some space, as we will outline in the next section. The relation between l^* , β^* and magnet aperture will be discussed in more detail in section 2.5. Moreover, the luminosity increase due to the reduction of the beam size in the interaction point is limited by the crossing angle and by the geometric reduction factor F (see Eq. 2.1). This will be discussed in section 2.4.

Limitations due to the number of events per crossing (aka pile-up). It is defined as the number of events that take place at the same time in the detector, and is given by the luminosity times the cross-section, divided by the revolution frequency and the number of bunches:

$$p_u \equiv \frac{L}{n_b f_{rev}} \sigma_{in}. \quad (2.20)$$

The challenge for the detector hardware and for the analysis software is to be able to separate the different events. In the nominal LHC the pile-up is ~ 20 , i.e., 20 events are present at the same time in the detector traces. To limit the pile-up keeping a large luminosity one has to increase the number of bunches (i.e., decrease the bunch spacing) rather than increase the number of particles per bunch. So the pile-up sets a limit on the “easy” way of increasing luminosity through increasing N_b . On the other hand, the increase of number of bunches is in conflict with the electron cloud requirements on the minimal bunch spacing.

2.3 Experiment requirements

The experimental magnets are spectrometers that bend the collision debris allowing to reconstruct the momentum/charge ratio from the deviation of the particle from a straight trajectory. There are different configurations, as a simple solenoidal field (see Fig. 2.2 left) or a toroidal field (see Fig. 2.2, center); here we will focus on the solenoidal configuration, that can be approximated by a constant magnet field parallel to the beam over a cylinder of radius R_t and semi-length l^* .

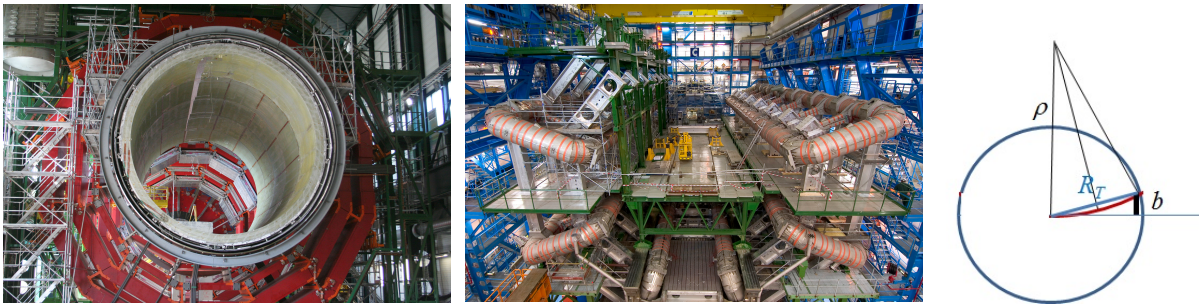


Fig. 2.2: the CMS solenoid (left) and the toroidal coils of ATLAS (center), and schematics of the trajectory of a charged collision debris (in red) in the plane transverse to the beam, where R_t is the experimental solenoid radius and ρ is the curvature radius induced by the solenoid magnetic field.

As shown in the previous chapter, a charged collision debris, with momentum p in the plane transverse to the beam, will be curved by the magnetic field of the solenoid B on a curvature radius ρ according to

$$p = eB\rho. \quad (2.21)$$

Assuming that the particle is perpendicular to the beam trajectory, it will reach the outer radius of the detector solenoid R_T with a deviation b from the straight trajectory (see Fig. 2.2, right). Since the 90° triangles made with b and R_T , and made with $R_T/2$ and ρ are similar, one has

$$\frac{b}{R_T} = \frac{R_T/2}{\rho} \quad b = \frac{R_T^2}{2\rho} = \frac{eBR_T^2}{2p} = 0.15 \frac{BR_T^2}{E[\text{GeV}]} \quad (2.22)$$

Therefore, the precision in measuring the particle momentum is proportional to R_T^2/B : to improve the precision it is much more effective to increase the detector transverse radius than its magnetic field. This is the reason behind experimental detector sizes of the order of 10 m. To have the same deviation b with the same particle energy, reducing the radius of a factor ten would require increasing the magnetic field by a factor 100.

Example 2.6: In the ALEPH experiment [8] we have a solenoid with 1.5 T magnetic field and 2.65 m radius and 6.5 m longitudinal length. What is the deviation b for a 115 GeV particle at the exit of the solenoid?

$$b = 0.15 \frac{BR_T^2}{E[\text{GeV}]} = 0.15 \frac{1.5 \times 2.65^2}{115} = 13.7 \text{ mm} \quad (2.23)$$

So considering a resolution in the detector of 0.1 mm, one can measure the momentum with 1% precision.

Example 2.7: Use a scaling of ALEPH detector to propose a solenoid for the LHC.

Since the energy increase is 61 (from 115 GeV to 7 TeV), we can share this increase between a factor 3 in the magnetic field (i.e. going to 4.5 T) and the remaining factor $61/3 = 20$ should be covered by a factor ~ 4.5 increase in solenoid radius, i.e. from 2.65 m to 12 m.

Example 2.8: In LHC we have a distance of the first magnet to the interaction point $l^* = 23$ m. What could be used for the FCC, which has a ~ 7 times larger energy?

Since $7^{1/3} = 1.9$, one can use a 1.9 larger radius (and length of the experiment), and a 1.9 larger magnetic field. Therefore, $l^* \sim 23 \times 1.9 = 44$ m, and the field in the solenoid would increase from 4 T to 8 T.

2.4 Separation and recombination dipoles for colliders with two beam pipes

We have shown in Chapter 1 that a collider based on two beams of identical particles require two beam pipes, with the main dipole fields in opposite direction. Until LHC, the magnetic system of a collider was based on independent magnets for each beam pipe. In the LHC, the design has been based on a dipole providing opposite field in two apertures, separated by a minimal distance (~ 200 mm) sufficient to avoid a large electromagnetic coupling between the two beam pipes. In both cases, the beams travel in separate apertures along most of the accelerator and then they are put on the same path via a separation and a recombination dipole [2], as shown in Fig. 2.3. The recombination dipole is a double aperture dipole, with field in the same direction, making converge the beams up to the separation dipole, where they get a second dipolar kick to place them on the same path towards the experiment. After the separation dipole one has the triplet of quadrupoles, i.e. the magnets closer to the experiment. In Section 2.6 we will show the interest in placing the triplet as close as possible to the experiment to get the smallest possible beam size in the collision point without requiring too large apertures for the magnets. Other layouts are possible, as placing the dipoles closer to the experiment, and then the quadrupoles (dipole-first [9] layout), but are less effective in reducing the IP beam size.

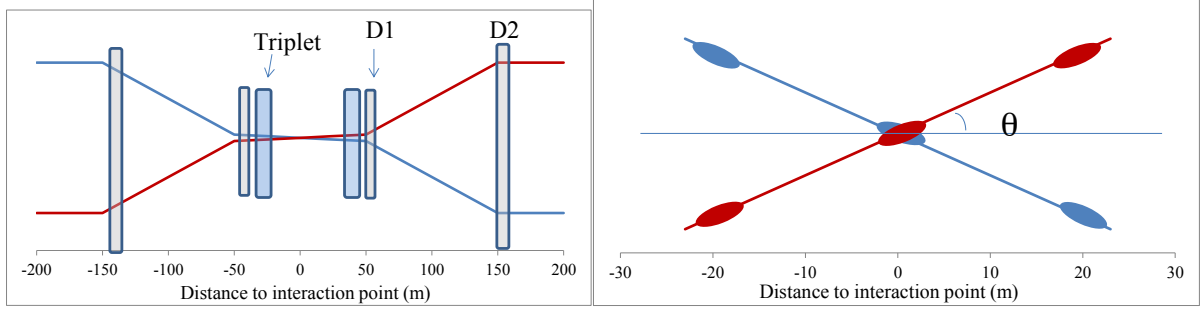


Fig. 2.3: Schematic of the orbit in a layout with a triplet, a separation D1 and a recombination D2 dipole (left) and magnification of the crossing angle around the interaction point (right).

Example 2.9: The integrated field of the separation and the recombination dipole in the LHC around ATLAS and CMS is 27 T m at 7 TeV energy. Compute the angular kick given by each dipole, and the distance between the baricentre of the dipoles knowing that the beam interdistance is 192 mm.

Since the curvature radius of LHC is 2808 m and the dipole field is 8.3 T, the integrated required field to have a 2π rotation is $2 \times \pi \times 2808 \times 8.3 = 146$ kT m. Therefore 1 mrad kick is given by $146/2\pi = 23.3$ kT m. Since the dipole have a 27 T m integrated field, they will change the beam angle trajectory by $27/23.3 = 1.16$ mrad. This kick shall displace the beam by half of the distance between the beam apertures in the arc, i.e. $192/2 = 96$ mm. Therefore the distance between the D1 and D2 baricentre shall be $96/1.16 = 82$ m.

Example 2.10: In FCC-hh collider [6], with 50 TeV beam energy, the beam separation is 250 mm. Assuming a distance between D1 and D2 of 100 m, estimate the integrated field in D1 and D2.

The dipole kick should be $250/2/100 = 1.25$ mrad (not far from the LHC values). For a 50 TeV collider as FCC-hh, 1 mrad kick is given by

$$1 \text{ mrad} = \frac{\rho B}{1000} = \frac{E [\text{GeV}]}{1000 \times 0.3} = \frac{50}{0.3} = 167 \text{ T m} . \quad (2.25)$$

Therefore the integrated field of the separation/recombination dipoles shall be $167 \times 1.25 = 208$ T m. Using Nb-Ti, with a 8 T field one could use two units of 13-m-long dipoles.

2.5 Crossing angle and geometric reduction factor

When the bunch spacing is smaller than the longitudinal size of the experiment, one has to avoid the collisions taking place not in the center of the detector (usually called parasitic collisions). For instance, in the LHC the bunch spacing is 7.5 m, the longitudinal size of the experiments is $2l^* = 46$ m, so one has six additional points inside the experiment where bunches collide. The solution is to have the beams colliding not exactly face to face, but with a small crossing angle θ (see Fig. 2.3, right).

Let us require that the separation of the beams at a distance s of the interaction point is equal to n sigma of the beam (for the LHC one takes $n \sim 10$)

$$2s\theta = n \sqrt{\frac{\epsilon_n \beta(s)}{\gamma_r}} . \quad (2.26)$$

Since close to the interaction point the beta function behaves as s^2/β^* (see Eq. 2.19), one has

$$2s\theta = n \sqrt{\frac{\varepsilon_n s^2}{\beta^* \gamma_r}} \quad \theta = \frac{n}{2} \sqrt{\frac{\varepsilon_n}{\beta^* \gamma_r}} \quad (2.27)$$

so to keep this distance between the beams, the crossing angle has to scale with the inverse of the square root of β^* .

The crossing angle gives a reduction of the luminosity of a factor F (see Eq. 2.1) given by

$$F(\theta) = \sqrt{\frac{1}{1 - \left(\frac{\sigma_z \theta}{\sigma_x}\right)^2}} \approx \sqrt{\frac{1}{1 - \frac{\gamma_r}{\varepsilon_n \beta^*} \left(\frac{\theta}{2\sigma_x}\right)^2}} \quad (2.28)$$

where σ_z is the longitudinal length of the bunch. Here we do not give any proof of this equation: this reduction is due to the fact that the bunches are not colliding head on, and therefore the area where the beam intersect is reduced by the crossing angle (see Fig. 2.3, right). At the same time, the reduction of β^* requires a larger crossing angle as given in (2.27) to avoid parasitic collisions. One can observe that in the limit of small β^* (i.e. very large magnet aperture close to the interaction regions), the geometric factor becomes proportional to β^*

$$F(\theta) = \sqrt{\frac{1}{1 - \frac{\gamma_r}{\varepsilon_n \beta^*} \left(\frac{\theta}{2\sigma_x}\right)^2}} \xrightarrow{\beta^* \rightarrow 0} \beta^* . \quad (2.29)$$

In this limit, the F factor perfectly compensates for the luminosity increase proportional to $1/\beta^*$, the positive effect of reducing β^* vanishes and luminosity saturates at a constant value. In Fig. 2.4 we give the dependence of crossing angle and geometric reduction as a function of β^* , and the values chosen for the LHC operation. Note that the use of crab cavities [3] allow to tilt the bunches and collide them head on even with a nonzero crossing angle, i.e., to remove the geometric reduction factor. This option will be implemented in the LHC upgrade, aiming at a strong reduction of β^* .

Example 2.11: Compute the crossing angle for the LHC, for the HL-LHC project [10] and for the FCC study, requiring a 10 sigma separation.

For the LHC one has

$$\theta = \frac{10}{2} \sqrt{\frac{3.75 \times 10^{-6}}{0.55 \times 7450}} = 150 \mu\text{rad} . \quad (2.30)$$

The four times smaller beta function, foreseen for HL-LHC, gives a twice larger crossing angle:

$$\theta = \frac{10}{2} \sqrt{\frac{3.75 \times 10^{-6}}{0.15 \times 7450}} = 290 \mu\text{rad} . \quad (2.31)$$

The crossing angle proportional to the inverse of the square root of the energy. Therefore for a case as the FCC-hh study, having 50 TeV beam energy and a $\beta^* = 0.3$ m, the crossing angle can be smaller

$$\theta = \frac{10}{2} \sqrt{\frac{3.75 \times 10^{-6}}{0.3 \times 53200}} = 77 \mu\text{rad} . \quad (2.32)$$

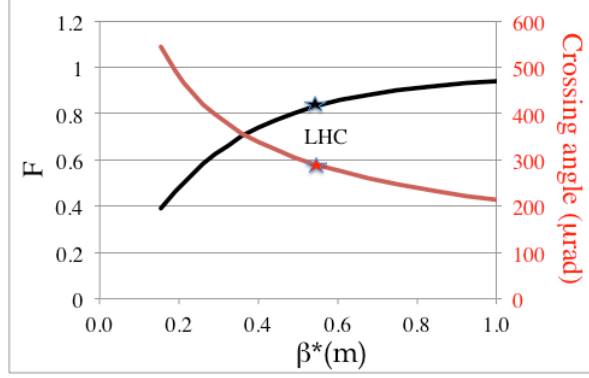


Fig. 2.4: Dependence of the crossing angle and of the geometric reduction factor on β^* , and the case of the LHC

2.6 Optics around the interaction regions and triplet requirements

As outline in Section 2.2, and discussed in more detail in Appendix A.7, in a region free of magnetic field the beta function is quadratic in the longitudinal coordinate:

$$\beta(s) = \beta^* + \frac{s^2}{\beta^*} \quad (2.33)$$

where s is the distance along the beam axis to the interaction point, and β^* is the beta function in the interaction point. The consequence of this equation is that to obtain small β^* , the size of the beam in the first magnet placed after the experimental area at a distance l^* from the interaction point, becomes very large (see Fig. 2.5)

$$\beta(l^*) = \beta^* + \frac{l^{*2}}{\beta^*} \approx \frac{l^{*2}}{\beta^*}. \quad (2.34)$$

The final focus quadrupoles are used to bend the parabolic beta functions in the experiment and to bring them down to values that can be matched to the beta functions in the arcs. To give an order of magnitude in the LHC, l^* is 23 m, nominal β^* is 0.55 m, and using (2.34) $\beta^*(l^*)$ is 1050 m, whereas in the arc it ranges between 30 and 170 m. The reduction of these large beta functions at the boundary of the experiment is done through a series of quadrupoles (3 in the LHC); one needs at least two quadrupoles to focus the beam in both planes, since a single quadrupole is focusing in one plane but defocusing in the other one. A triplet configuration F-D-F is very effective to steer the beta functions down to matchable values for the arc, and it is shown in Fig. 2.5 for the LHC case.

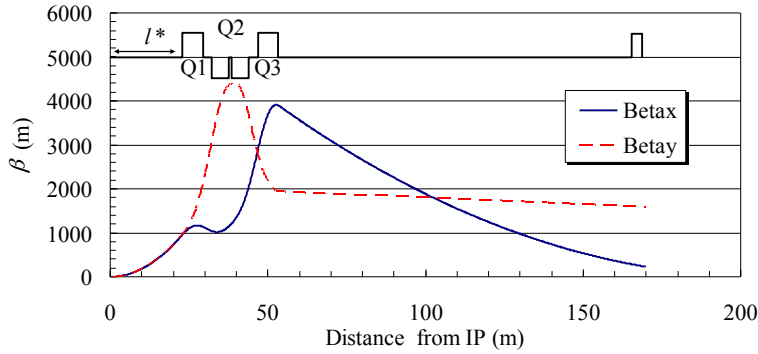


Fig. 2.5: Beta functions close the LHC interaction point, and position of the triplet and of the quadrupole Q4.

In a triplet the focusing force is approximately $(-f, 2f, f)$ and having the same gradients in each quadrupole, the ratio between the lengths of Q1/Q3 and Q2 is around a factor 2. Q2 is usually split in two magnets, giving the paradox that a triplet is usually composed of four magnets. The ratio between the Q1/Q3 length and the Q2 length is used to fine tune the values of the maximum beta function in both planes, making them equal, so to best exploit the precious magnet aperture. This optimal ratio is related to the gaps between the magnets, to the total length of the triplet l_t , and to l^* . Note that in the LHC baseline shown in Fig. 2.5 this optimization is not perfectly realized since the gaps between magnets were changed after setting the quadrupole lengths.

What is the required focusing strength of the quadrupole triplet? Keeping the optics analogy, one has

$$\frac{Gl_q}{B\rho} = \frac{1}{f} \approx \frac{1}{l^*} \quad (2.35)$$

and therefore for the whole triplet

$$Gl_t \approx \frac{4B\rho}{l^*}. \quad (2.36)$$

For instance, in the LHC one has Q1 and Q3 length of 6.23 m, and Q2 of 11 m, split in two 5.5-m-long magnets, with a 200 T/m gradient. This gives an integrated gradient of 4700 T, to be compared to the right-hand side of (2.38) that gives 1000 T.

$$Gl_t = 200 \times (6.23 \times 2 + 11) = 4700 \text{ T} \quad \frac{4B\rho}{l^*} = \frac{4 \times 8.3 \times 2808}{23} = 4070 \text{ T}. \quad (2.37)$$

However, the maximum beta function is much larger than the beta function at the entrance of the Q1 given by Eq. (2.35) as the triplet is far from being a thin lens: in the LHC case shown in Fig. 2.5 the total length of the triplet (23.5 m) is similar to the distance to the interaction point (23 m). Therefore the scaling of (2.36) can be improved to

$$Gl_t \approx \kappa \frac{4B\rho}{l^* + \frac{l_t + l_g}{2}}. \quad (2.38)$$

where l_g is the total length of gaps in the triplet, and the additional factor in the denominator accounts for the real baricentre of the triplet, and κ accounts for the deviations from thin lens optics, with $\kappa \sim 1.8$ in the range $l^* < l_t < 2l^*$.

Note that when the beam is injected, the optical functions in the interaction points are kept at values which are close to the minimum beta function in the arcs. After the acceleration to nominal energy, the β^* is squeezed, i.e., it is reduced to its nominal value (needed for producing a large luminosity). During the squeeze, the gradient of the triplet is constant, since as discussed in this chapter and more in detail in the Appendix A, according to the optics analogy, the gradient is given by the triplet focal length; the squeeze is performed using the quadrupoles in the matching section and in the dispersion suppressor, that lay between the triplet and the arcs. Therefore one the following statements are true:

- Increasing the triplet gradients does not further reduce β^* , but just makes the triplet “astigmatic”, i.e. the optics is not closed and the beam does not circulate any more;
- If the triplet does not reach the nominal gradient the optics cannot be produced at any β^* , and the only way to have circulating beams is to reduce the beam energy;
- When the triplet aperture is at the limit of the beam size imposed by β^* , any further reduction of β^* has to go through a larger triplet aperture increase, and not through a larger gradient.

We can now define an algorithm to estimate a layout around the interaction point, and its minimum β^* .

- Select a distance between the IP and the first quadrupole l^* , according to the requirements of the experiments.

- Select the triplet length l_t and the length of the gaps l_g between the magnets. The triplet length together with the magnet technology will give the β^* at the end of the process. Then, one can select a longer length to increase β^* or a shorter length to reduce it, and iterate the process.
- Having fixed the layout, one can estimate the ratio r between the maximum beta function in the triplet and the beta function at the entrance of the triplet. This gives the maximum beta function in the triplet.

$$\beta_{\max} = r \frac{l_t^2}{\beta^*}. \quad (2.39)$$

Since the triplet is thick, r is larger than one. When the triplet length is between l^* and $2l^*$ one has the approximate relation

$$r \approx 1 + a \frac{l_t}{l^*}. \quad (2.40)$$

with $a \sim 3.6$ for gaps of the order of 1 m. This means that if the triplet length is equal to the distance of the first magnet to the interaction point, as in the LHC, the beta function inside the triplet is ~ 4.6 times larger than the beta function at the entrance.

- The optics computation also gives the required gradient G to match the optics according to the scaling given in Eq. (2.38). For longer l^* and for longer l_t , the required integrated gradient becomes smaller.
- Select a magnet technology: this will give the maximum triplet aperture ϕ that is possible to achieve through the equation

$$\lambda \frac{G\phi}{2} < B_t \quad (2.41)$$

where B_t is the maximum field provided by the technology. The peak field is given by the gradient times the aperture radius, plus an additional term λ accounting for the overshooting of the peak field in a quadrupole (this issue is discussed in detail in Section 8.8, and in typical cases is $\lambda \sim 1.15$).

- We can now compute the minimum β^* by equating the aperture given by Eq. (2.43) to the aperture requirements given by Eq. (1.52) in Chapter 1.

$$\frac{\phi}{2} = n \sqrt{\frac{\epsilon_n \beta_{\max}}{\gamma_r}}. \quad (2.42)$$

This intricate set of equations and constraints will become more clear in the following examples.

Example 2.12 (LHC case): In the LHC [2], the distance of the triplet to the interaction point is $l^* = 23$ m. The triplet is made by Q1 and Q3, whose length is 6.3 m, and Q2 is split in two magnets of 5.5 m. The triplet coils have a 70 mm aperture. Compute: (i) the quadrupole gradient and check if it can be in Nb-Ti, (ii) the maximum beta function in the triplet for a β^* of 0.55 m, (iii) the aperture required by the beam assuming that the triplet must house two beams of 10 sigma, separated by 15 sigma. (iv) Is there enough space in the magnet to reach $\beta^* = 0.25$ m? (v) If not, can you reach it by reducing the emittance by 30%?

(i) The length of the triplet is $l_t = 6.3 \times 2 + 11 = 23.6$ m, and applying Eq. (2.38) we obtain

$$Gl_t \approx k \frac{4B\rho}{l^* + \frac{l_t}{2}} = 1.8 \frac{4 \times 8.3 \times 2808}{23 + \frac{23.6}{2}} = 4820 \text{ T} \quad G \approx \frac{4820}{23.6} = 205 \text{ T/m} \quad (2.43)$$

The peak field is estimated using (2.41):

$$B_t = \lambda \frac{G\phi}{2} = 1.15 \times 205 \times 0.035 = 8.3 \text{ T} . \quad (2.44)$$

So the coil is at the limit of the Nb-Ti technology, whose operational fields should not exceed 8.5-9 T.

(ii) The maximum beta function is given by (2.39)

$$\beta_{\max} = r \frac{l^{*2}}{\beta^*} = \left(1 + a \frac{l_t}{l^*}\right) \frac{l^{*2}}{\beta^*} = \left(1 + 3.6 \frac{23.6}{23}\right) \frac{23^2}{0.55} = 4400 \text{ m} . \quad (2.45)$$

(iii) The required aperture of $10+15+10=35$ sigma is

$$\phi = n \sqrt{\frac{\epsilon_n \beta_{\max}}{\gamma_r}} = 35 \sqrt{\frac{3.75 \times 10^{-6} \times 4400}{7450}} = 52 \text{ mm} . \quad (2.46)$$

So the beam fits within the 70 mm aperture of the magnet.

(iv) If we decrease β^* to 0.25 m, β_{\max} increases to 9700 m according to (2.39), and the now beams requires an aperture of

$$\phi = n \sqrt{\frac{\epsilon_n \beta_{\max}}{\gamma_r}} = 35 \sqrt{\frac{3.75 \times 10^{-6} \times 9700}{7450}} = 77 \text{ mm} \quad (2.47)$$

so the beam does not fit in the 70 mm magnet aperture.

(v) If the beam emittance is reduced from 3.75 to 2.2×10^{-6} m, then

$$\phi = n \sqrt{\frac{\epsilon_n \beta_{\max}}{\gamma_r}} = 35 \sqrt{\frac{2.2 \times 10^{-6} \times 9700}{7450}} = 59 \text{ mm} \quad (2.48)$$

and therefore $\beta^*=0.25$ m can be achieved; this configuration was used in the RunII of the LHC.

Example 2.13 (LHC upgrade with Nb-Ti): Consider a new layout of the LHC interaction region with longer magnets, $l_{Q1}=l_{Q3}=9.2$ m and $l_{Q2a}=l_{Q2B}=7.8$ m, based on Nb-Ti [11]. Compute (i) the quadrupole gradient, (ii) the aperture that can be provided by Nb-Ti technology and (iii) the minimum β^* that can be reached, assuming that the magnet aperture must exceed the 35 sigma by 20%.

(i) The length of the triplet is $l_t=9.2 \times 2 + 7.8 \times 2 = 34$ m, plus 3 m for gaps, and applying Eq. (2.16) we obtain

$$G \approx \frac{k}{l_t} \frac{4B\rho}{l^* + \frac{l_t + l_g}{2}} = \frac{1.8}{34} \frac{4 \times 8.3 \times 2808}{23 + \frac{34 + 3}{2}} = 123 \text{ T/m} \quad (2.49)$$

(ii) Assuming a 8.5 T peak field, the maximum aperture is:

$$\phi = \frac{2B_t}{\lambda G} = \frac{2 \times 8.5}{1.15 \times 123} = 120 \text{ mm} . \quad (2.50)$$

(iii) The requirement on the aperture is to have 20% more than 35 sigma:

$$\phi = 1.2 \times 35 \sqrt{\frac{\epsilon_n \beta_{\max}}{\gamma_r}} \quad (2.51)$$

and therefore the maximum β_{\max} is

$$\beta_{\max} = \frac{\gamma_r}{\varepsilon_n} \left(\frac{\phi}{1.2 \times 35} \right)^2 = \frac{7450}{3.75 \times 10^{-6}} \left(\frac{0.120}{1.2 \times 35} \right)^2 = 16200 \text{ m}. \quad (2.52)$$

Using Eq. (2.34) one can compute the β^* reach

$$\beta^* = r \frac{l^{*2}}{\beta_{\max}} = \left(1 + a \frac{l_t}{l^*} \right) \frac{l^{*2}}{\beta_{\max}} = \left(1 + 3.6 \frac{34}{23} \right) \frac{23^2}{16200} = 0.021 \text{ m}. \quad (2.53)$$

The above exercise shows a fundamental feature of the triplet optics: *given a magnet technology, one can always reach lower β^* by making the triplet longer, larger and with smaller gradient.*

Example 2.14 (HL-LHC case): consider a new layout of the LHC interaction region in Nb₃Sn, assuming 11.5 T operational peak field and a 150 mm aperture [10]. Compute (i) the gradient and the triplet length, (ii) the minimum β^* that can be reached, assuming that the magnet aperture must exceed the 35 sigma by 20%.

The gradient is given by Eq. (2.43)

$$G = \frac{2B_t}{\lambda\phi} = \frac{2 \times 11.5}{1.15 \times 150} = 133 \text{ T/m}. \quad (2.54)$$

To estimate the triplet length one has to invert Eq. (2.16)

$$Gl_t = k \frac{4B\rho}{l^* + \frac{l_t}{2}} \quad (2.55)$$

$$l_t = \frac{-2l^* + \sqrt{(2l^*)^2 + 32kB\rho/G}}{2} = \frac{-46 + \sqrt{46^2 + 32 \times 1.8 \times 8.3 \times 2808/133}}{2} = 32 \text{ m} \quad (2.56)$$

and verify a posteriori that the application range of (2.38) $l^* < l_t < 2l^*$ is satisfied. The β_{\max} is

$$\beta_{\max} = \frac{\gamma_r}{\varepsilon_n} \left(\frac{\phi}{1.2 \times 35} \right)^2 = \frac{7450}{3.75 \times 10^{-6}} \left(\frac{0.150}{1.2 \times 35} \right)^2 = 25400 \text{ m}. \quad (2.57)$$

and the minimum β^* is

$$\beta^* = r \frac{l^{*2}}{\beta_{\max}} = \left(1 + a \frac{l_t}{l^*} \right) \frac{l^{*2}}{\beta_{\max}} = \left(1 + 3.6 \frac{30}{23} \right) \frac{23^2}{25400} = 0.12 \text{ m}. \quad (2.58)$$

Example 2.15: Consider the layout of the FCC-hh interaction region [6], with 50 TeV energy, and 62 m distance between the interaction point and the first triplet magnet. Estimate the triplet length and gradient for a 140 mm aperture, assuming a Nb₃Sn technology with 12 T peak operational field, and compute the β^* reach.

The gradient is given by Eq. (2.43)

$$G = \frac{2B_t}{\lambda\phi} = \frac{2 \times 12}{1.15 \times 0.140} = 150 \text{ T/m}. \quad (2.59)$$

To estimate the triplet length one has to invert Eq. (2.16) as in the previous case

$$l_t = \frac{-2l^* + \sqrt{(2l^*)^2 + 32kB\rho/G}}{2} = \frac{-62 + \sqrt{62^2 + 32 \times 1.8 \times 16 \times 10400/150}}{2} = 98 \text{ m}. \quad (2.60)$$

With such a long triplet, the magnets will be split in several units. The β_{max} can be estimated as

$$\beta_{max} = \frac{\gamma_r}{\varepsilon_n} \left(\frac{\phi}{1.2 \times 35} \right)^2 = \frac{53200}{3.75 \times 10^{-6}} \left(\frac{0.140}{1.2 \times 35} \right)^2 = 157 \text{ km}. \quad (2.61)$$

and the minimum β^* is

$$\beta^* = r \frac{l^{*2}}{\beta_{max}} = \left(1 + a \frac{l_t}{l^*} \right) \frac{l^{*2}}{\beta_{max}} = \left(1 + 3.6 \frac{98}{62} \right) \frac{62^2}{157000} = 0.16 \text{ m}. \quad (2.62)$$

Acknowledgements

I wish to thank J. P. Koutchouk for introducing me to the beam optics in the interaction regions, and for the preparatory work done together for the LHC upgrade.

References

1. A. Chao, M. Tigner, "Handbook of accelerator physics and engineering" World Scientific, Singapore (1999)
2. O. Bruning, et al., "LHC design report" [CERN-2004-003 \(2004\)](#)
3. S. Holmes, R. Moore and V. Shiltsev, "Overview of Tevatron collider complex: goals, operations and performance" [J. Instrum. 6 \(2011\)](#)
4. M. Lamont, "Status of the LHC" [J. Phys.: Conf. Series 455 \(2013\) 012001](#)
5. F. Zimmermann, et al., "Review of single bunch instabilities driven by electron cloud" [Phys. Rev. ST Accel. Beams 7 \(2004\) 124801](#)
6. A. Abada, et al., "FCC-hh: the hadron collider" [Eur. Phys. J. Spec. Top. 228 \(2019\) 755-1107](#)
7. A.A.V.V. "LEP design report, v.2: the main ring" [CERN-LEP-84-01 \(1984\)](#)
8. J. M. Baze, et al., "Design, construction and test of the large superconducting solenoid ALEPH" [IEEE Trans. Magn. 24 \(1988\) 1260-1263](#)
9. O. Bruning, et al., "LHC luminosity and energy upgrade: a feasibility study" [LHC project report 626 \(2002\) p. 27](#)
10. O. Aberle, et al., "HL-LHC technical design report" [CERN-2020-010 \(2020\)](#)
11. J. P. Koutchouk, L. Rossi, E. Todesco, "A solution for phase-one upgrade of the LHC low-beta quadrupoles based on Nb-Ti" [LHC project report 1000 \(2007\)](#)